# Comparison of the Response of a Homogeneous Medium to the Dynamic Impact of Single and Segmented Rods

**Alexander E. Kraus**\*
**Ivan I. Shabalin**†
**Andrey E. Buzyurkin**‡
**Evgeny I. Kraus**§
Khristianovich Institute of Theoretical and Applied Mechanics SB RAS
Novosibirsk, Russian Federation

**Abstract.** A series of calculations of the interaction of single and segmented rods with massive blocks and plates of finite thickness have been performed. Comparisons with experimental data for verification of material parameters under dynamic conditions have been made. Both qualitative and sufficiently realistic correspondence of the results of numerical modeling to the experimental data, such as the non-monotonic dependence of the cavity depth of segmented rods on the size of the gap between the segments, has been obtained.

**Keywords:** fracture, impact, numerical simulation.

## Introduction

It is known experimentally that the cavity depth in a massive, semi-infinite block from the impact of a segmented rod (two or more rods on the same axis flying in series) is greater than the cavity depth from the impact of a single rod with the same mass and velocity. It should be noted that, in general, single rods are tested on plates of finite thickness [1, 2, 3]. In this paper, the interaction of rods with both finite thickness plates and massive blocks is considered.

Let us consider some comparative studies of the ballistic efficiency of single and segmented rods in interaction with massive blocks. Thus, in [4], a series of experiments were conducted to evaluate the characteristics of rods striking targets with velocities two to three times higher than normal impact velocities. The results were positive: rods with a low $L/D$ ratio (length/diameter) exceeded the theoretical hydrodynamic penetration limit for the rod-massive block combination. Rods with a high $L/D$ ratio did not exceed this limit. A second series of experiments was designed to test the hypothesis that a segmented rod consisting of a set of low $L/D$ rods assembled in

\*akraus@itam.nsc.ru      https://orcid.org/0000-0002-2426-0558
†shabalin@itam.nsc.ru    https://orcid.org/0000-0002-4447-2558
‡buzjura@itam.nsc.ru     https://orcid.org/0000-0001-8164-8789
§kraus@itam.nsc.ru        https://orcid.org/0000-0001-5478-1293

a long rod configuration could form a crater with greater depth than a single rod of equivalent mass. The results were also positive, with gains of up to 10% in some cases.

An analytical model was proposed in [5], with the help of which the authors determined with acceptable accuracy the forces at the interface between an impacting rod and a massive block, the penetration velocities of single and segmented rods, and the crater depth. It was found that at high velocities, the effectiveness of the segmented rod is higher than that of the single rod. Moreover, it was found that the penetration depth of the segmented rod is directly proportional to the gaps between the segments and the number of segments for velocities greater than 3 km/s.

In [6], the effectiveness of segmented rods penetrating massive steel objects was also shown using numerical simulations at impact velocities from 2 to 5 km/s. The experiments performed with segmented rods confirmed the numerical simulation results. The results showed an increase in penetration depth of about 10% when using a rod with four segments at an impact velocity of 2.1 km/s.

In [7], numerical modeling of penetration of a rod with elongation equal to 5 and segmented impactors into steel solid blocks was carried out. The Lagrangian approach with the Johnson–Cook hardening model was used in the modeling. The analysis showed that the dominant contribution to the penetration depth of the segmented rod is due to the initial unsteady stage rather than the final quasi-steady stage of the penetration, which dominates the penetration by the single rod. The authors paid special attention to the effect of segment length and spacing on penetration depth. The results of the study showed that the aspect ratio and the distance between segments do not affect the penetration depth.

In [8], numerical modeling of the processes of high-velocity impact of segmented rods on massive blocks was considered. The study was carried out by comparing the penetration velocity of a segmented rod and a single rod of the same mass and diameter. The results showed that the segmented rod has an advantage over the single rod in almost the whole range of velocities from 1 to 12 km/s.

In [9], on the basis of numerical simulations in two-dimensional axisymmetric formulation, the peculiarities of the process of penetration into a massive steel block of segmented and single rods of high-density alloy at interaction velocities from 1.4 to 2 km/s were analyzed. In the framework of the study, for segmented rods, the dependence of the penetration depth increment on the distance between neighboring segments along the direction of their motion and on the number of segments at their fixed total length has been established. The achievable increment of penetration depth into a steel block, compared to an equivalent single rod of the same mass and length, was fixed at 20%.

In [10], for rods with velocities from 2 to 7 km/s, it was shown that the crater depth can be more than doubled by segmenting the rod.

The question of the optimal arrangement of segments in a segmented rod remains open, since the penetration depth also depends on the distance between the segments. In the study [11], a comparison of the penetration depth into a solid block was performed. The effectiveness of segmented rods was related to the general mathematical properties of the penetration models. The developed approach was applied to high-velocity interaction. It was shown that the gain or lack of gain from segmentation can be predicted if the function describing the segmentation is convex and satisfies a certain inequality at the left endpoint of the interval. The authors of [11] demonstrated that the penetration depth increases as the number of segments increases with equal segment length and gaps between segments.

Based on the above, let us compare the results of the high-velocity impact of a single rod and

a set of segments of the same mass with semi-infinite blocks and plates of finite thickness.

# 1. Problem statemenent

Numerical calculations of the process of high-velocity interaction of solid bodies were performed by the program complex "REACTOR 3D" [12]. In which the equations of mass, momentum, and energy balance are realized in the Lagrangian formulation: the particle trajectory equation $\dot{x}_i = u_i$,

the mass balance equation $V_0 \rho_0 = V \rho$,

the momentum balance equation $\rho \dot{u}_i = \sigma_{ij,j}$,

the internal energy balance equation $\rho \dot{e} = \sigma_{ij} \dot{\varepsilon}_{ij}$,

the strain rate tensor $\dot{\varepsilon}_{ij} = \frac{1}{2}\left(u_{i,j} + u_{j,i}\right)$,

the stress tensor $\sigma_{ij} = -\delta_{ij}P + s_{ij}$,

where $x_i$ and $u_i$ are the components of the position and velocity vectors of a material particle, respectively; $\rho$ is the current density; $s_{ij}$ is the stress deviator, which characterizes the shear-induced change in the shape of a material particle; $\delta_{ij}$ is the Kronecker symbol. $P$ is the pressure function in the form of Mie–Grüneisen.

The elastoplastic flow equations are formulated in the form of Prandtl–Reuss equations

$$\hat{s}_{ij} + d\lambda' s_{ij} = 2G\dot{\varepsilon}'_{ij}, \dot{\varepsilon}'_{ij} = \dot{\varepsilon}_{ij} - \dot{\varepsilon}_{kk}/3,$$

with the Huber–von Mises plasticity condition $s_{ij} \cdot s_{ij} \leqslant 2 \cdot Y_0^2/3$, where $G$ is the shear modulus; $Y_0$ is the dynamic yield stress. Instead of calculating the scalar factor $d\lambda'$, we use the well-known procedure of reducing the stress deviator components to the yield circle. In the equations above, each of the subscripts $i, j$ takes values 1, 2, and 3; summation is performed over repeating indices; a dot above a symbol denotes the time derivative, and a subscript after a comma denotes the derivative with respect to the corresponding coordinate.

The partial derivative equations are transformed into an explicit difference scheme on triangular (2D) and tetrahedral (3D) meshes along the trajectory of each material particle. The difference mesh in arbitrary multi-connected regions is constructed in a dynamic manner [13, 14]. The computational regions are shown in Fig. 1.
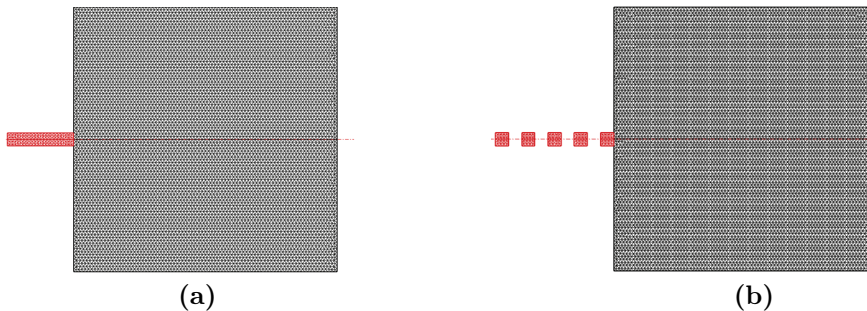


**(a)**                      **(b)**

Fig. 1. Geometric model of interaction with a massive block: (a) single rod; (b) segmented rod

To account for fracture processes, the system is supplemented with relations linking the parameters of the stress-strain state with the limiting values of materials [15]. The thermodynamically complete low-parameter equation of state [16, 17] is used as the equation of state,

which is characterized by the fact that almost all parameters can be found in reference books on the physical and mechanical properties of materials. The calculation of contact surfaces between interacting deformable solids is carried out using a symmetric algorithm [15].

Application of the "REACTOR 3D" program complex allows solving problems of deformable solid mechanics in a wide range of encounter velocities [18, 19, 20].

## 2.  Results of calculations of rod penetration into solid blocks

Following the work [21], let's delve into the interaction process between a tungsten alloy W10 rod and a large steel block made of 4340 steel. The rod's geometric properties include a length ($L$) of 5 cm, a diameter ($D$) of 1 cm, and an elongation ratio ($L/D$) of 5. For the segmented rod, the mass characteristics remain similar, with each element measuring 1 cm in length and a 1 cm gap between segments.

Regarding the massive steel block, its geometric parameters entail a radius of 10 cm and a thickness of 20 cm. The collision velocity between the two bodies is 2.55 km/s.

This stage of calculation serves as a verification phase. All computations are conducted within the two-dimensional axisymmetric approximation. Based on experiments and computations detailed in [15, 21], a sequence of numerical calculations concerning the aforementioned processes has been executed, utilizing the material parameters outlined in Tab. 1.

Table 1. Material parameters

| Material | $\rho$, g/cm$^3$ | $G$, GPa | $K$, GPa | $Y_0$, GPa | $\sigma_*$, GPa | $\varepsilon_*$ | $\varepsilon_t$ | $\chi^*$, % |
|---|---|---|---|---|---|---|---|---|
| W10 | 17.0 | 160 | 311 | 0.645 | 2 | 0.35 | 0.25 | 4 |
| Steel 4340 | 7.85 | 75 | 183 | 1 | 7.5 | 0.25 | 0.2 | 3 |

The results of calculations and experimental data are compiled in Tab. 2. Numerical calculations, based on the parameters from Tab. 1, exhibited a strong correlation with the experimental results. As anticipated, a segmented rod delivers the maximum depth of penetration into a solid block. Fig. 2 illustrates the penetration outcome of the segmented rod at an impact velocity of 2.55 km/s.

Table 2. The results of the interaction between rods and massive steel blocks

| Crater depth $h$, cm | Experiment [22] | Calculation [15] | Author's calculation |
|---|---|---|---|
| single rod | 4.1 | 4.59 | 4.24 |
| segmented rod | 4.6 | 5.24 | 4.63 |

Subsequently, let's explore the impact of the number of segments in the segmented rod on its penetration depth into an infinite block. To achieve this, a 5 cm long rod was segmented into N parts, with each segment placed at intervals equivalent to the length of one segment, while maintaining the fundamental condition of equal kinetic energy within the rod, similar to a solid one. For instance, with 5 segments, each segment's length equals 1 cm, and the distance between segments also measures 1 cm. Therefore, the number of rod segments varied from 1 to 10 in the scenarios under examination. The results of the numerical calculations, demonstrating the
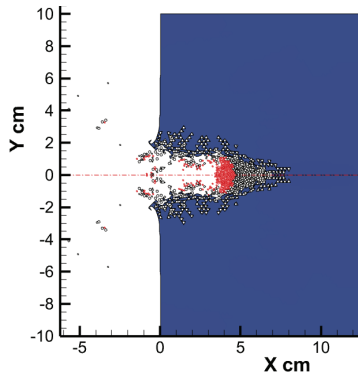
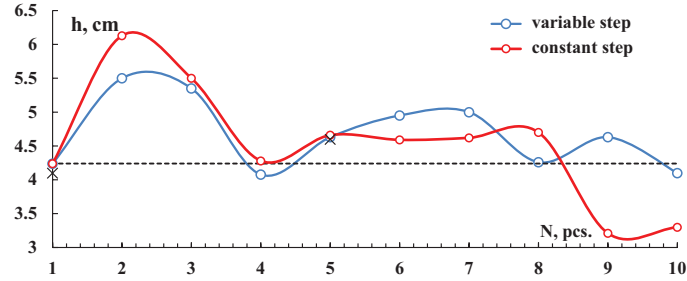Fig. 2. Segmented rod penetration into a massive block



Fig. 3. The dependence of the penetration depth of a segmented rod on the number of segments

magnitude of the crater depth relative to the number of segments, are shown in Fig. 3. The dots represent calculated results for a given number of segments, while the dashed line indicates the penetration depth of a single rod.

The calculations revealed that the maximum crater depth is achieved with a segmented rod configuration consisting of two elements. Conversely, the shallowest crater depth was observed in the configuration with a four-segment rod. However, a similar penetration pattern was evident when maintaining a consistent spacing between the segmented rod elements. This consistent spacing, equivalent to a rod diameter of 1 cm, was consistent with the spacing used in a five-segment rod.

In such a segmented rod configuration, reducing the number of elements led to shorter lengths and reduced spacing between them. This resulted in an outcome akin to that achieved by a single rod, as illustrated in Fig. 4a when ten elements were arranged in segmented rod. Notably, in a segmented rod with a consistent spacing, once the number of elements surpassed 8 units, there was a significant decrease in penetration depth, demonstrated in Fig. 4b for a ten-element rod.



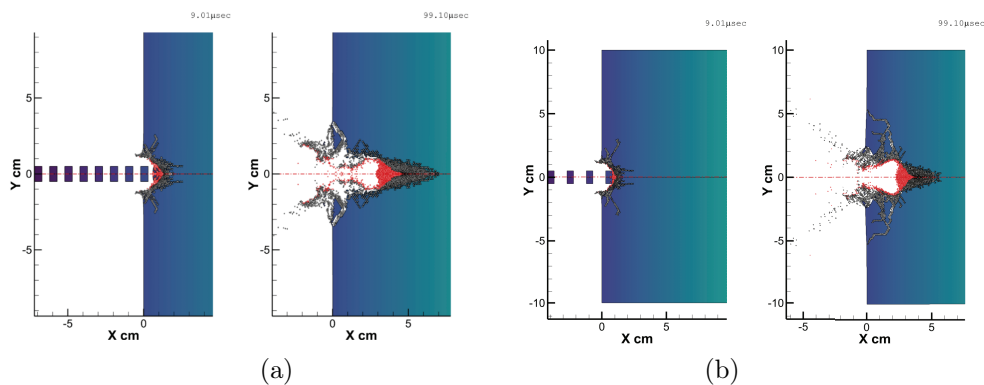(a)                                              (b)

Fig. 4. The process of interaction of 10 segments with a plate of finite thickness at a velocity of 2.55 km/s. The gap is equal to: (a) the length of the segment; (b) the diameter of the segment

Let's explore how the gap size between segments affects the depth of penetration into a solid block. In study [4], the assumption, derived from extrapolating experimental data, suggested an increase in penetration depth as the gap between segments widened from one to three times the
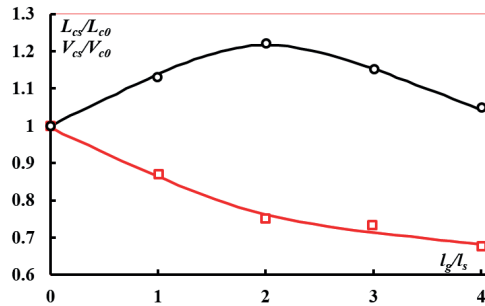
Fig. 5. The relationship between relative penetration depth (squares) and relative cavity volume (circles)

diameter of the rod. However, study [6] conducted numerical simulations based on experiments from [22], considering various gap sizes between segments. The results demonstrated a non-monotonic relationship for interaction velocities around 2 km/s, reaching a peak when the gap size equaled the diameter of the segments. It's worth noting that the experiment involved four segments.

The results presented in Fig. 5 demonstrate the modeling of the penetration process of single and segmented rods into a solid block using relative units $L_{cs}/L_{c0}$ from $l_g/l_s$. Here, $L_{c0}$ and $L_{cs}$ represent the cavity depth caused by the single and segmented rods, 'g' denotes the gap size between segments, and 'l' signifies the segment length. As shown in Fig. 5, the relationship between the relative penetration depth and the gap size between segments is non-monotonic, in alignment with the findings from experiments [22].

The maximum penetration depth occurs when the gap between segments $l_g$ is equivalent to twice the segment length. This is because the subsequent segment comes into contact with the preceding one when their velocities align at the specific flight velocity of the segments. With a further increase in the gap between segments $l_g$, interactions happen between a segment approaching its predecessor with opposing velocities, leading to deceleration and thus reducing the cavity depth. Despite the increased cavity depth $L_{cs}$, its volume $V_{cs}$ decreases due to the reduced diameter compared to the volume of a cavity $V_{c0}$ in a single rod. The subsequent decrease in cavity volume is linked to reductions in both its depth and diameter (refer to Fig. 5).

The interaction calculations of the segmented rod were performed in both a two-dimensional axial setup and a three-dimensional arrangement. The calculation results, shown in Fig. 6, illustrate the comparable processes of deformation and failure between the segmented rod components and the material of the solid block.

## 3.    Penetration of finite thickness plates

Next, we will compare the results of the penetration of plates with finite thickness using single and segmented rods in a 3D case. The parameters of the rods, both in terms of their geometry and material properties, are akin to the ones mentioned earlier. The thickness of the 4340 steel plate ranges from 1 to 5 cm. It's important to note that due to the problem's symmetry, it is possible to conduct calculations for a quarter of the interacting bodies, imposing symmetry conditions at the cut boundaries. This significantly reduces the time required for the computations. The geometric model of a quarter of the body is shown in Fig. 7, with red lines indicating the planes of sliding.
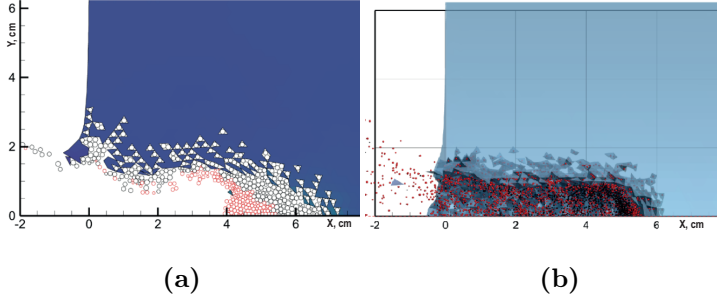
**(a)**          **(b)**

Fig. 6. Penetration results into a solid block by a segmented rod at a velocity of 2.55 km/s: (a) 2D axial simulation; (b) 3D simulation
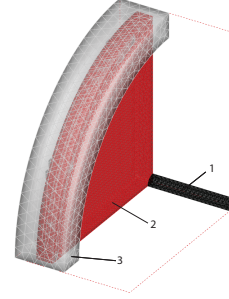
Fig. 7. 3D model of a quarter of the computational area: 1 — rod; 2 — steel plate; 3 — guard ring

The deterministic approach to establishing the ballistic limit involves attempting to predict the rod's behavior during penetration by developing models founded on conservation laws and assumptions about the mechanical properties of interacting bodies. Based on extensive experimental data analysis by Lambert and Jonas, an empirical formula for calculating the residual velocity was proposed and subsequently generalized as follows [23]:

$$u_{\text{res}} = \chi \left( u_{\text{imp}}^p - u_{\text{bal}}^p \right)^{1/p}, \quad u_{\text{imp}} > u_{\text{bal}}, \tag{1}$$

where $u_{\text{imp}}$, $u_{\text{res}}$, $u_{\text{bal}}$ represent impact velocity, residual velocity, and ballistic velocity magnitude, while $\chi$, $p$ are constants dependent on the properties of materials and the geometry of the colliding objects.

Derived from [24], a formula has been obtained for the modeled rod-plate configuration to estimate the ballistic velocity of penetrating a plate with a finite thickness

$$u_{\text{bal}} = \sqrt{\frac{2 \left( \rho_p L_p + \rho_t h_t \alpha^2 \right)}{\left( \rho_p L_p R_p \right)^2} \left[ \left( \sigma_t \varepsilon_t h_t \left( \alpha R_p \right)^2 \right) \left( b + c_1 \left( \frac{h_t}{R_p} \right)^{c_2} \right) \right]}, \tag{2}$$

where rod parameters: $\rho_p$ is the density, $R_p$ is the radius, $L_p$ is the length; plate parameters: $\rho_t$ is the density; $\sigma_t$ is the ultimate spall strength; $\varepsilon_t$ is the ultimate shear strain; $h_t$ is the thickness; $\alpha$, $b$, $c_1$, $c_2$ are empirical coefficients. For the 4340 steel plate, the coefficient values are as follows: $\alpha = 2.51$, $b = 0.96$, $c_1 = 4.62$, $c_2 = -0.7$.

From a series of numerical experiments conducted, it was observed that with small plate thicknesses (where the plate's thickness is less than the rod's length), both segmented and single rods exhibit identical residual velocities. Additionally, the ultimate ballistic velocities are also equivalent, as shown in Fig. 8a. However, as the plate thickness increases, a distinction emerges between the residual velocities and the ultimate ballistic velocities. Specifically, the single rod commences plate penetration at an interaction velocity of 1.5 km/s, whereas the segmented rod initiates plate penetration at 1.6 km/s. Notably, the segmented rod, upon penetration, displays a slightly higher residual velocity, as clearly illustrated in Fig. 8b.

The comparison between the results obtained from numerical calculations and those derived from formula (2) is outlined in Tab. 3. The accuracy in predicting the ballistic velocity is attributed to the inclusion of mechanical parameters of both the rod and plate materials within formula (2), with free parameters selected from a singular reference point.
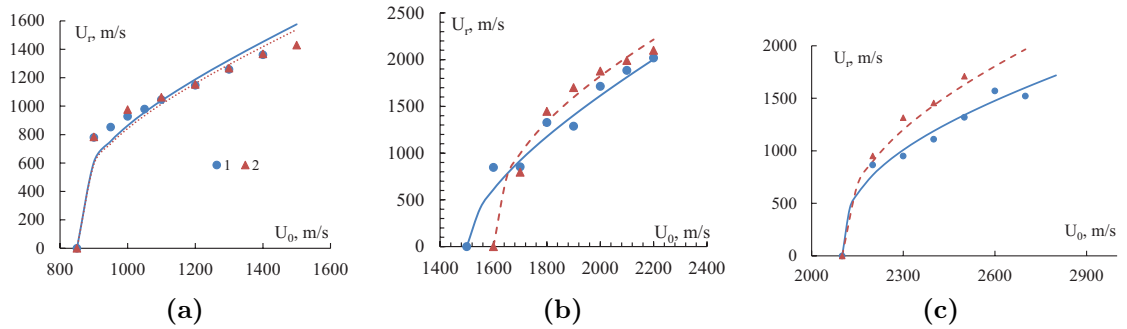
Fig. 8. Ballistic penetration curves for plates of finite thickness: (a) 1 cm; (b) 3 cm; (c) 5 cm. Calculation results: 1 — single rod; 2 — segmented rod; lines represent the approximate ballistic curves derived using Lambert's formula (1)

Table 3. The relationship between ballistic velocity and plate thickness

| Plate thickness $h$, cm | 1 | 2 | 3 | 5 |
|---|---|---|---|---|
| Ballistic velocity $u_{\text{bal}}$, km/s | 0.850 | 1.25 | 1.50 | 2.10 |
| Estimation by formula (2) $u_{\text{bal}}$, km/s | 0.849 | 1.18 | 1.49 | 2.07 |

In assessing the effectiveness of segmented rods compared to a single rod on thick plates, let's examine the state of the rods at the moment of complete penetration, as shown in Fig. 9. The plate thickness is 2 cm, and the interaction velocity is 1.5 km/s. At this juncture, the segmented rod retains only two segments, or approximately 40% of the initial mass, while the residual mass of the single rod is about 50%. Interestingly, their residual velocities are nearly equal.
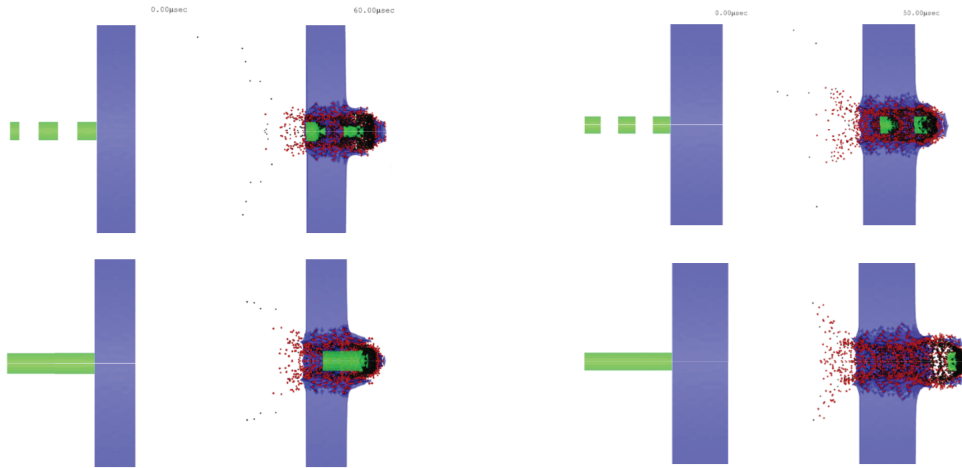


Fig. 9. The penetration process of a 2 cm thick plate using a segmented rod (top) and a single rod (bottom) at a velocity of 1.5 km/s

Fig. 10. The penetration process of a 3 cm thick plate using a segmented rod (top) and a single rod (bottom) at a velocity of 2.0 km/s

An increase in plate thickness and the resulting collision velocity provide an advantage to segmented rods over single rods in terms of residual mass and velocity, as shown in Fig. 10.

The plate thickness is 3 cm, and the interaction velocity is 2 km/s. At the point of complete penetration, the segmented rod retains two segments, while the single rod retains about 20% of its initial mass, presenting roughly a twofold advantage in residual mass. The residual velocity of the segments is approximately 1.89 km/s, compared to the residual velocity of the fragment from the single rod, which is about 1.72 km/s. This supports the efficacy of segmented rods as plate thickness increases.

Let's examine the penetration of a 5 cm thick plate by a segmented rod at a velocity of 2.3 km/s. It's important to note that the chosen final plate thickness exceeds the crater depth in an infinite block at an interaction velocity of 2.55 km/s with a segmented rod consisting of 10 elements at a consistent interval (refer to Fig. 3). As illustrated in Fig. 11, this velocity is entirely adequate for complete penetration of a thicker plate. This occurrence is attributed to the influence of the free surface and the formation of a spall 'dish' on the rear side of the plate, reducing its resistance.
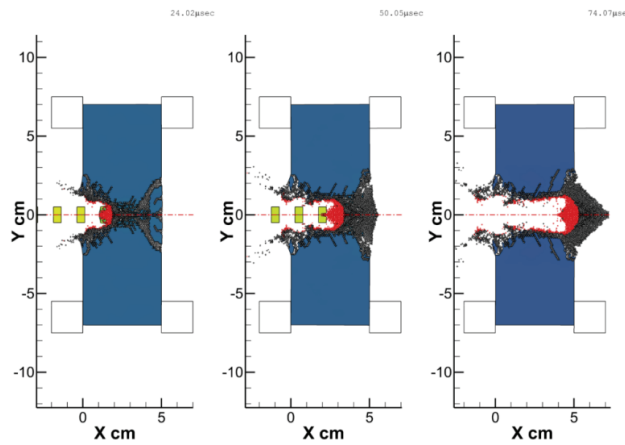


Fig. 11. Penetrating a 5 cm thick plate at a velocity of 2.3 km/s with a segmented rod

# Conclusion

1. Segmented rods demonstrate higher efficiency compared to single rods of similar mass when penetrating semi-infinite blocks across the entire range of velocities examined.

2. Similar to experimental findings, a non-linear relationship was observed between the depth of the cavity created by the segmented rod and the gap size between segments. It was determined that the cavity depth depends on the materials of the rod, the solid block, and their interaction velocity.

3. Segmented rods outperform single rods of the same mass in residual velocity during the complete penetration of finite-thickness homogeneous plates, with their effectiveness increasing as the plate thickness rises.

# References

[1] A.M.Bragov, A.Yu.Konstantinov, A.K.Lomunov, Experimental-Theoretical Investigation of High-Velocity Deformation and Fracture Processes of Materials of Different Physical Nature Using the Kolsky Method and Its Modifications, NNSU, N. Novgorod, 2018.

[2] P.A.Radchenko, S.P.Batuev, A.V.Radchenko, *Russ. Phys. J.*, **64**(2021), 811. DOI 10.1007/s11182-021-02396-1

[3] P.A.Radchenko, S.P.Batuev, A.V.Radchenko, *J. Eng. Phys. Thermophys.*, **95**(2022), 90. DOI: 10.1007/s10891-022-02457-3

[4] J.H. Cuadros, *Int. J. Impact Eng.*, **10**(1990), 147.

[5] K.M.Moustafa, A.M Riad, M.S.Abdel-Kader, In Proccetlings 8th Int. AMME Conf., 1998, 131–147.

[6] P.Naz, H.F.Lehr, *Int. J. Impact Eng.*, **10**(1990), 413.

[7] X.W.Chen, L.Lang, *Struct. Under Shock Impact XIII*, (2014), 125–137. DOI: 10.2495/SUSI140111

[8] E.N.Kramshonkov, A.V.Krainov, P.V.Shorohov, *MATEC Web Conf.*, **72**(2016), 01051. DOI: 10.1051/matecconf/20167201051

[9] S.V.Fedorov et al., *Vestn. Mosk. Gos. Tekh. Univ. im. N.E. Baumana, Mashi- nostr.*, **3(108)**(2016), 100–117. DOI: 10.18698/0236-3941-2016-3-100-117

[10] S.V.Fedorov, *Vestn. N. Nov. Univ.ersity im. N.I. Lobachevsky*, **4**(2011), 1819–1821 (in Russian).

[11] G.Ben-Dor, A.Dubinsky, T.Elperin, *Mech. Based Des. Struct. Mach.*, **38**(2010), 372.

[12] A.E.Kraus, E.I.Kraus, I.I.Shabalin, In: Behav. Mater. under Impact, Explos. High Press. Dyn. Strain Rates, Springer International Publishing, Vol. 176, 2023, 83–101.

[13] E.I.Kraus, V.M.Fomin, I.I.Shabalin, *Comput. Technol.*, **11**(2006), 104.

[14] E.I.Kraus, V.M.Fomin, I.I.Shabalin, *Comput. Technol.*, **14**(2009), 40.

[15] V.M.Fomin et al., High-Velocity Solids Interaction, SB RAS, Novosibirsk, 1999 (in Russian).

[16] E.I.Kraus, V.M.Fomin, I.I.Shabalin, *Fiz. Mezomekh.*, **7**(2004), 285.

[17] E.I.Kraus, I.I.Shabalin, *AIP Conf. Proc.*, **2125**(2019), 030065. DOI: 10.1063/1.5117447

[18] E.I.Kraus et al., *J. Appl. Mech. Tech. Phys.*, **60**(2019), 526. DOI: 10.1134/S0021894419030155

[19] M.Yu.Fedorov et al., *Vestnik Mosk. Aviats. In-Ta*, **16**(2009), 49.

[20] A.Kraus et al., *Appl. Sci.*, **13**(2023), 7187.

[21] P.M.Holland et al., *Int. J. Impact Eng.*, **10**(1990), 241.

[22] E.Wollmann et al., ISL – Report No. S-RT 906/88, 1988.

[23] J.A.Zukas, T.Nicholas, H.F.Swift, L.B.Greszczuk, D.R.Curran, Impact Dynamics, Wiley, New York, 1982.

[24] A.Serjouei et al., *Procedia Eng.*, **75**(2014), 14.  DOI: 10.1016/j.proeng.2013.11.003

# Сравнение реакции гомогенной среды на динамическое воздействие одиночного и сегментированного стрежней

**Александр Е. Краус**
**Иван И. Шабалин**
**Андрей Е. Бузюркин**
**Евгений И. Краус**
Институт теоретической и прикладной механики им. С. А. Христиановича СО РАН
Новосибирск, Российская Федерация

**Аннотация.** Выполнены серии расчетов взаимодействия сплошных и сегментированных стержней с массивными блоками и пластинами конечной толщины. Проведены сравнения с данными экспериментов для верификации параметров материалов в динамических условиях. Получено как качественное, так и достаточно реалистичное соответствие результатов численного моделирования данным экспериментов, таких как немонотонная зависимость глубины каверны сегментированных стержней от величины зазора между сегментами.

**Ключевые слова:** разрушение, удар, численное моделирование.